

Gate-controlled transport in narrow GaAs/Al_xGa_{1-x}As heterostructures

H. Z. Zheng,* H. P. Wei, and D. C. Tsui

Department of Electrical Engineering, Princeton University, Princeton, New Jersey 08544

G. Weimann

Forschungsinstitut der Deutschen Bundespost, D-6100 Darmstadt, West Germany

(Received 23 May 1986)

The transport of two-dimensional electrons in the narrow channel, realized by the split gate of a GaAs/Al_xGa_{1-x}As heterojunction field-effect transistor, is investigated from 4.2 to 1.3 K as a function of the gate voltage V_g . Results from Shubnikov-de Haas effect and low-field magnetoresistance measurements show that the channel width W and the electron density n_s decrease linearly with V_g and that the mobility μ decreases with n_s to the power $\frac{3}{2}$. The phase-breaking length l_i in the one-dimensional weak-localization regime is studied as a function of V_g . We find that the functional dependence of l_i on the channel conductance is in good agreement with theory.

There has been in recent years a great deal of interest in the physics of electronic transport in ultrasmall structures. The dimensionality of the electronic system defined by such small structures, a most important parameter to characterize the electron physics, is determined by the various pertinent length scales in the physics of the underlying electronic process. Most experimental investigations of transport in one-dimensional (1D) systems have thus far been carried out on low mobility systems, such as polycrystalline metal films¹⁻³ and Si MOSFET's (silicon metal-oxide-semiconductor field-effect transistors).⁴⁻⁷ The length scales of interest are typically in the range of or less than a few hundred angstroms and the structures are usually fabricated by using electron-beam lithography and ion-etching processes, known to degrade high mobility electronic materials. Only recently a series of experiments were performed on the high mobility two-dimensional electron gas (2D EG) in GaAs/Al_xGa_{1-x}As heterostructures to study systematically the influence of the sample size on the quantum corrections to its Boltzmann transport.⁸ Dimensional crossover from 2D to 1D and to zero dimension was observed and the relevant length scales were demonstrated for both the localization and the electron-electron interaction effects in these experiments. Since the electron mobility is high and the length scales relevant to the physics of these electronic processes are in the order of micrometers, the sample structures are fabricated by simple mesa pattern definition, using photolithography and chemical etching to preserve the high electron mobility. However, it is apparent that this straightforward technique for fabricating small structures, though most reliable in preserving the high mobility of the 2D EG, is limited to micrometer-size features and not suitable for much smaller structures.

Several years ago, Fowler, Hartstein, and Webb⁴ introduced a technique for producing a 1D conducting channel by electric field pinching of the 2D EG in the accumulation layer of a Si MOSFET, using two reversed biased p - n junctions as side gates. The effective width of the 1D channel can be continuously varied by varying the reverse

bias on the side gates. We have adopted this technique and obtained, by using a pair of Schottky barrier junctions as side gates, a gate-controlled 1D conducting channel from the 2D EG in GaAs/Al_xGa_{1-x}As heterostructures. We fabricated the metal gates with micrometer-size separation, using photolithography and chemical etching, and thus preserved the 2D EG mobility of the starting material. The 1D conducting channel, resulting from the 2D EG in the gap between the side gates after the underneath 2D EG was completely depleted, can be continuously narrowed by further increasing the reverse bias V_g . We have studied the Shubnikov-de Haas effect of the channel and its low-field negative magnetoresistance due to 1D localization. We found that both the effective channel width W , and the areal density n_s , of the 2D EG decrease linearly with V_g and that the channel mobility μ decreases with n_s to the power $\frac{3}{2}$, as expected from scattering dominated by ionized impurities. Moreover, we obtain directly, from the quantum corrections due to 1D localization, the electron phase-breaking length l_i , as a function of the channel conductance. In the range of T studied, W is larger than the characteristic length for electron-electron interactions of the 2D EG and the l_i is dominated by electron-electron scattering in the 2D limit. In fact, the experimental l_i in the entire range of W from 0.37 to 1.6 μm is 58% of that calculated from the 2D electron-electron scattering theory with no adjustable parameters. A note should be added. We learned, after the completion of this work, that a similar split-gate structure has been employed by Thornton *et al.*⁹ to produce 1D conduction in GaAs/Al_xGa_{1-x}As. They used electron-beam lithography and fabricated split gates with 0.6- μm gap separation. No dependence of n_s on V_g was observed in their work.

The inset of Fig. 1 illustrates a cross section of the device structure, which is a Hall bridge of a GaAs/Al_xGa_{1-x}As heterostructure. The conducting channel of the 2D EG, having a width $W_2 (= 9 \mu\text{m})$, is defined by a mesa pattern chemically etched into the semi-insulating GaAs substrate. The split gate is a 1000 Å

thick Au film deposited on top of the $\text{Al}_x\text{Ga}_{1-x}\text{As}$ surface with a gap $W_1 (= 1.6 \mu\text{m})$, fabricated by using standard photolithography and lift-off techniques. The gap has a width variation typically less than 5%. The resulting Schottky barrier gate shows no detectable leakage current, on the level of 1×10^{-9} A, with reverse bias up to $V_g = -5$ V. The 1D conducting channel is realized by reverse biasing the split gate to completely deplete the 2D EG underneath it and the resulting channel width W can then be reduced by pinching it with further increase of V_g . This is apparent in the data shown in Fig. 1(a), which shows the channel resistance R_c obtained from four-terminal measurements, as a function of the reverse bias. This sample has $n_s = 3 \times 10^{11} \text{ cm}^{-2}$ and $\mu = 2.9 \times 10^4 \text{ cm}^2/\text{V sec}$. The observed increase in R_c with increasing V_g up to $V_g \sim -0.3$ V is due to depletion of the 2D EG underneath the split gate and the further increase in R_c beyond $V_g \sim -0.3$ V is due to pinching of the 1D channel in the gap. The sudden change in the rate of increase of R_c at $V_g \sim -0.3$ V signals the complete depletion of the 2D EG underneath the split gate.

The increase in the 1D channel resistance can in general result from decreases in W , n_s , and μ . The decrease of n_s accompanying pinching of the channel, is apparent in Fig. 1(b), which shows the Shubnikov–de Haas effect in R_c versus B for several reverse biases, measured by using a lock-in amplifier operating at 14.5 Hz for reverse biases < 1 V and 3.5 Hz for > 1 V. In the bias range from $V_g = -0.3$ to -1.5 V, R_0 , the channel resistance at $B=0$, increases from 141 k Ω to 2.63 M Ω . The quantum oscillations in the entire bias range are regular and well resolved, indicative of a highly uniform conducting channel. The decrease in n_s with increasing V_g is seen as an increase in the oscillation period in $1/B$. The n_s , determined from these quantum oscillations, as a function of V_g is shown as the circles in Fig. 2. It is clear that it decreases linearly with the reverse bias following

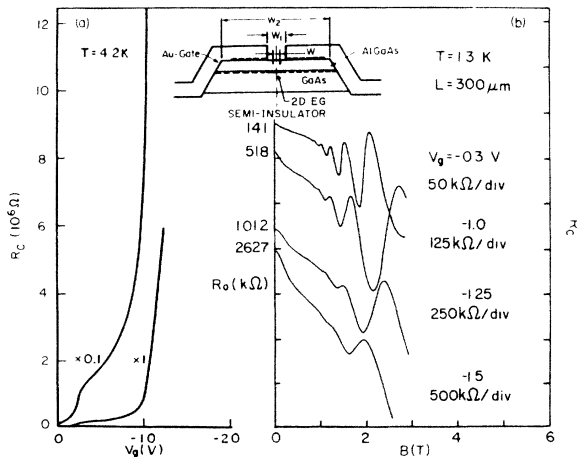


FIG. 1. (a) Channel resistance R_c as a function of gate voltage V_g at $T = 4.2$ K. The kink at $V_g \sim -0.3$ V indicates the complete depletion of electrons under the gate. (b) Shubnikov–de Haas oscillations for five different V_g at $T = 1.3$ K. The inset is a cross section of the split-gate configuration on the sample.

$$n_s = 3 \times 10^{11} - 1.07 \times 10^{11} (|V_g| - 0.3),$$

where V_g is in volts and n_s in cm^{-2} .

The bias dependence of the width W of the conducting channel is determined by studying the low-field magnetoresistance of the channel, due to weak localization,¹⁰ as a function of V_g . This negative magnetoresistance [we use $\Delta R \equiv R_0 - R(B)$], depends on the dimensionality of the electron system and is given by^{11–13}

$$\frac{\Delta R}{R_0} = R_0 \frac{W}{L} \frac{e^2}{2\pi^2 \hbar} \left[\psi\left(\frac{1}{2} + \hbar/4DeB\tau_i\right) - \psi\left(\frac{1}{2} + \hbar/4DeB\tau\right) - \ln\left(\frac{\tau_i}{\tau}\right) \right] \quad (1)$$

for 2D, and

$$\frac{\Delta R}{R_0} = \frac{R_0}{L} \frac{e^2}{\pi \hbar} \left[\left(\frac{1}{l_i^2} + \frac{W^2}{12l_B^4} \right)^{-1/2} - l_i \right] \quad (2)$$

for 1D. Here, ψ is the digamma function, L is the potential probe spacing, τ_i is the electron phase-breaking time related to l_i through $l_i = \sqrt{D\tau_i}$, and l_B is the magnetic length $l_B \equiv (\hbar/2eB)^{1/2}$. The elastic scattering time τ and the diffusion constant D are related to the channel conductance σ and the effective electron mass m^* through

$$\sigma = n_s e^2 \tau / m^* = e^2 D m^* / \pi \hbar.$$

The length scale determining the dimensionality of the system is l_i and it is now well known that the 2D to 1D crossover occurs when W becomes comparable to πl_i .

In Fig. 3, we show the low-field magnetoresistance data

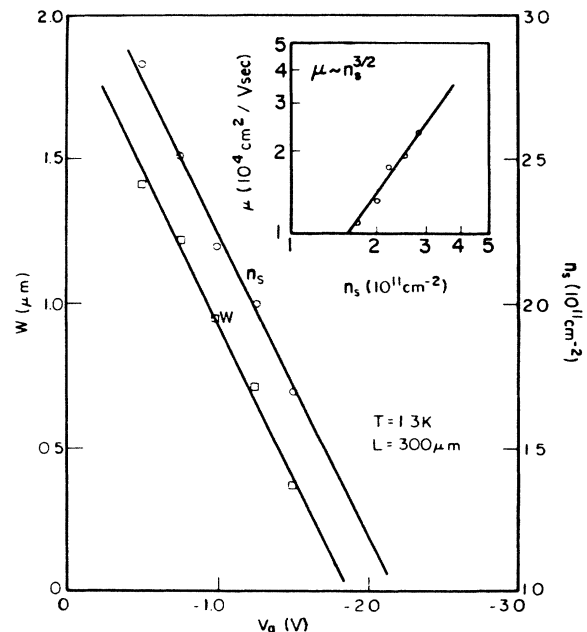


FIG. 2. Electron density n_s (\circ) and the effective channel width W (\square) as a function of V_g . The inset shows the mobility μ vs n_s .

at 1.3 K for V_g from -0.3 to -1.5 V. The data were taken with $I=1 \times 10^{-9}$ A to avoid electron heating, and were recorded using a computer system at a field interval $\Delta B \sim 0.5$ G. In Fig. 3, only a number of them were plotted to illustrate the theoretical fits. In the range of $B \leq 100$ G, where localization dominates the observed magnetoresistance and the electron-electron interaction effect is still negligible,¹⁴ we use the Nedler and Mead simplex algorithm¹⁵ to fit the data to Eq. (1), the 2D theory, and to Eq. (2), the 1D theory, with l_i and W as adjustable parameters. It turns out that, except for the $V_g = -0.3$ V data, the 1D theory gives a better fit to all the data, as expected, and the resulting fitting parameters, W and l_i , are physically reasonable. The solid curves in Fig. 3 show the overall fits; the fitting parameters W and l_i are listed in Table I and also are plotted as squares in Fig. 2 and as circles in Fig. 4. For $V_g = -0.3$ V, both the 2D and the 1D theory can fit the data and the fitting parameters are $W=1.61 \mu\text{m}$ and $l_i=0.906 \mu\text{m}$ from the 2D theory and $W=1.68 \mu\text{m}$ and $l_i=0.486 \mu\text{m}$ from the 1D theory. While W from both theories agrees with the measured gap width $W=1.6 \mu\text{m}$, l_i is considerably longer in the 2D fit.

The mobility of the conducting channel is obtained from R_0 and W and is plotted as a function of n_s in the inset of Fig. 2. Two remarks should be made. First, the density dependence of μ follows $\mu \propto n_s^{3/2}$. This result is consistent with the n_s dependence of the 2D EG in GaAs/Al_xGa_{1-x}As heterostructures at low T , when ionized impurity scattering dominates.¹⁶ Thus, the observed V_g dependence of μ results entirely from the decrease of n_s . It is thus clear that no additional scattering is introduced by V_g applied to the split gate and that the process-

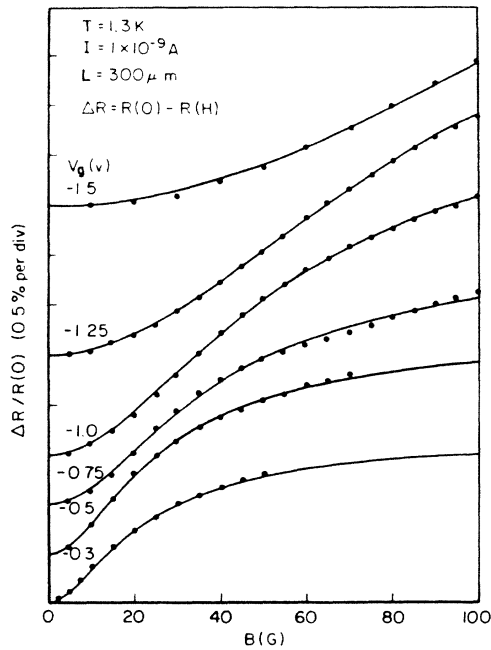


FIG. 3. Magnetoresistance as a function of B for different V_g at $T=1.3$ K. The solid circles are the data. The solid curves are obtained by fitting the data to Eq. (2). The fitting parameters W and l_i are given in Table I.

TABLE I. Fitting parameters.

V_g (V)	W (μm)	πl_i (μm)
-0.30	1.68	1.53
-0.50	1.41	1.44
-0.75	1.22	1.10
-1.0	0.94	0.96
-1.25	0.71	0.71
-1.50	0.38	0.52

ing steps, taken to fabricate the split-gate device, do not cause any degradation in the electron mobility. Second, W and n_s decrease linearly with V_g and W extrapolates to zero at $V_g \sim -1.9$ V, far below the gate breakdown expected above 5 V. It is interesting to note that as $W \rightarrow 0$, $n_s \rightarrow 1 \times 10^{11} \text{ cm}^{-2}$ and $\mu \rightarrow 10000 \text{ cm}^2/\text{V sec}$. Thus, there is no limit, in principle, to the width of the conducting channel that can be achieved by applying V_g . In practice, however, it will probably be limited by the fluctuations in the gap width of the split gate, which we estimate to be in the range of hundreds of angstroms. In this experiment, the narrowest conducting channel that we have demonstrated is $0.37 \mu\text{m}$ wide, achieved at $V_g = -1.5$ V. We are limited by our experimental setup to measure the channel resistance (to several times $10^6 \Omega$) and, at higher biases, the resistance is beyond our measuring capability. In fact, we use unnecessarily large potential probe separations ($L \sim 300 \mu\Omega$) in this experiment. It should be feasible to realize narrow conducting channels in the hundred-angstroms range and still be amendable to experimentation by simply reducing L to several microns.

In Fig. 4, we plot l_i versus the channel conductance $\sigma = (L/R_c W)$. We recall that l_i is the phase-breaking length of the 2D electrons, which, at the T (1.3 K) of our experiment, is determined by electron-electron scattering, and that σ is a measure of the disorder in the channel. Since the length parameter, $L_T = \pi(\hbar D/kT)^{1/2}$, relevant to electron-electron interactions is always smaller than W in our experiment, l_i is given by the 2D interaction theory through $l_i = (D\tau_i)^{1/2}$ and^{17,18}

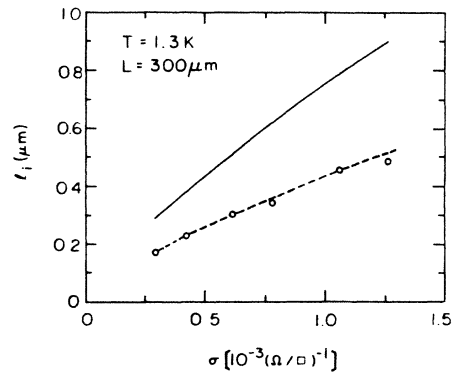


FIG. 4. Phase-breaking length l_i (\circ) as a function of the channel conductance σ . The solid curve is the theoretical value from Eq. (3). The dashed curve is 0.58 times the theoretical curve.

$$\frac{1}{\tau_i} = \frac{\pi}{2} \frac{(kT)^2}{\hbar E_F} \ln \frac{E_F}{kT} + \frac{kT}{2E_F \tau} \ln \frac{4E_F \tau}{\hbar}, \quad (3)$$

where $E_F = n_s \pi \hbar^2 / m^*$ and the electron effective mass in GaAs is $m^* = 0.067 m_0$. The T^2 term, from the momentum-conserving process, dominates when $T > \hbar / k\tau$ and the linear T term, from the momentum-nonconserving process, dominates when $T < \hbar / k\tau$. In our case, the two terms are comparable and the calculated l_i versus σ is shown as the solid curve in Fig. 4. It is interesting to note that while the experimental data lie consistently below the theoretical curve, the functional dependence of l_i on σ from theory is in excellent agreement with the experiment. This agreement is demonstrated by the dashed curve which is 0.58 times the theoretical curve. It should also be noted that, while the predicted functional dependence of l_i on T was observed in earlier experiments,^{1,19} our result is the first clear demonstration of the predicted functional dependence of l_i on σ , with both the T and the T^2 terms taken into account. In view of the perturbative nature of the electron-electron interaction theory, the small disagreement in magnitude is not unexpected.

In summary, we have fabricated split-gate GaAs/Al_xGa_{1-x}As heterojunction field-effect transistors to demonstrate the realization of gate-controlled narrow channels of the 2D EG in GaAs without degrading the electron mobility of the starting material. A systematic

investigation of the transport properties of the conducting channel from 4.2 to 1.3 K is carried out as a function of V_g . The results from the Shubnikov-de Haas effect and the low-field magnetoresistance measurements show that W and n_s decrease linearly with V_g and, while n_s and μ are still finite, W extrapolates to zero. Moreover, $\mu \sim n_s^{3/2}$ as expected for scattering dominated by ionized impurities at low T . We have not observed any additional degradation of the electron mobility by the applied V_g and it can be inferred that it is possible by this technique to produce narrow channels of extremely high mobility (several times 10^5 cm²/V sec) 2D EG in the range of several hundred angstroms, a width much smaller than the electron mean-free path and the de Broglie wavelength. We studied the low-field magnetoresistance due to weak localization in the 1D regime and extracted l_i as a function of V_g . The functional dependence of l_i on σ is found to be in excellent agreement with the theory for phase-breaking time of Altshuler, Aronov, and Khmelnitsky,¹⁷ when both the momentum-conserving and momentum-nonconserving electron-electron scattering processes are taken into account.

We thank K. K. Choi, M. J. Chou, and M. Frei for discussions. The work at Princeton University is supported by the U.S. Army Research Office through Contract No. DAAG29-85-K0098 and the U.S. Office of Naval Research through Contract No. N00014-82-K-0450.

*Present address: The Institute of Semiconductors, Academia Sinica, Beijing, China.

¹P. Santhanam, S. Wind, and D. E. Prober, Phys. Rev. Lett. **53**, 1179 (1984).

²J. L. Licini, G. J. Dolan, and D. J. Bishop, Phys. Rev. Lett. **54**, 1585 (1985).

³R. A. Webb, S. Washburn, C. P. Umbach, and R. B. Laibowitz, Phys. Rev. Lett. **54**, 2696 (1985).

⁴A. B. Fowler, A. Hartstein, and R. A. Webb, Phys. Rev. Lett. **48**, 196 (1982).

⁵W. J. Skocpol, L. D. Jackel, E. L. Hu, R. E. Howard, and L. A. Fetter, Phys. Rev. Lett. **49**, 951 (1982).

⁶R. G. Wheeler, K. K. Choi, A. Goel, R. Wisnieff, and D. E. Prober, Phys. Rev. Lett. **49**, 1674 (1982).

⁷C. C. Dean and M. Pepper, J. Phys. C **17**, 5663 (1984).

⁸K. K. Choi, D. C. Tsui, and S. C. Palmateer, Phys. Rev. B **32**, 5540 (1985); **33**, 8216 (1986).

⁹T. J. Thornton, M. Pepper, H. Ahmed, D. Andrews, and G. J. Davies, Phys. Rev. Lett. **56**, 1198 (1986).

¹⁰See, for example, the review by P. A. Lee and T. V. Ramakrishnan, Rev. Mod. Phys. **57**, 287 (1985).

¹¹B. L. Altshuler, D. Khmelnitsky, A. I. Larkin, and P. A. Lee, Phys. Rev. B **22**, 5142 (1980).

¹²B. L. Altshuler and A. G. Aronov, Pis'ma Zh. Eksp. Teor. Fiz. **33**, 515 (1981) [JETP Lett. **33**, 499 (1981)].

¹³H. Fukuyama, Surf. Sci. **113**, 489 (1982).

¹⁴B. J. Lin, M. A. Paalanen, A. C. Gossard, and D. C. Tsui, Phys. Rev. B **29**, 927 (1984).

¹⁵J. A. Nedler and R. Mead, Comput. J. **7**, 308 (1965).

¹⁶D. C. Tsui, G. Kaminsky, and W. Wiegmann, Appl. Phys. Lett. **39**, 712 (1981); B. J. F. Lin, D. C. Tsui, M. A. Paalanen, and A. C. Gossard, *ibid.* **45**, 695 (1984).

¹⁷B. L. Altshuler, A. G. Aronov, and D. E. Khmelnitsky, J. Phys. C **15**, 7367 (1982).

¹⁸H. Fukuyama and E. Abrahams, Phys. Rev. B **27**, 5976 (1983); H. Fukuyama, J. Phys. Soc. Jpn. **53**, 3299 (1984).

¹⁹K. K. Choi, Phys. Rev. **28**, 5774 (1983).